Estimation of a Lyapunov-exponent spectrum of plasma chaos

W. Huang,[1] W. X. Ding,[1,2] D. L. Feng,[1] and C. X. Yu[1]

[1]Department of Modern Physics, University of Science and Technology of China, Hefei, 230026, People's Republic of China

[2]China Center of Advanced Science and Technology (World Laboratory),
P.O. Box 8730, Beijing 100080, People's Republic of China

A practical algorithm is presented to obtain a reliable estimation of Lyapunov exponents from a time series signal of plasma chaos. In particular, the effect of inevitable experimental noise on the computation of Lyapunov exponents has been investigated. A full Lyapunov-exponent spectrum has been achieved to confirm transition from quasiperiodicity to chaos in a plasma.

PACS number(s): 05.45.+b, 52.35.Ra

I. INTRODUCTION

The deterministic chaotic behavior of nonlinear dynamical systems has become a very interesting subject in many fields of science. In particular, plasma, as one of the most attractive nonlinear systems, can exhibit not only chaotic behavior with a few degrees of freedom, but also spatiotemporal irregular behavior (turbulence). Recently, some experiments have been reported on chaotic behavior occurring in driven and undriven plasma [1–3]. Three important routes to chaos, i.e., period doubling, intermittent, and quasiperiodic chaos, are observed in these experiments. The power spectrum, phase portrait, Poincaré section, universal constants, and correlation dimension have been applied to these experiments to characterize chaotic behavior. However, there exist strange nonchaotic attractors in some dynamical systems [4]; therefore, to verify the existence of chaos quantitatively and especially to identify periodic, quasiperiodic, and chaotic attractors, a Lyapunov-exponent spectrum is required. The Lyapunov-exponent spectrum provides a quantitative measure of the sensitive dependence on initial conditions, and provides a classification of dynamics systems. Once Lyapunov exponents can be determined, the Lyapunov dimension (also called the Kaplan-Yorke fractal dimension D_{KY}) and Kolmogorov-Sinai entropy can be estimated as equalities and upper bounds [5–7]. Since the connection among transport properties, Lyapunov exponents, and entropy per unit time has been discussed recently [8], some transport properties might be estimated from Lyapunov exponents and KS entropy in experiments and it is possible that transport properties in fusion plasma could be investigated by means of a Lyapunov-exponent spectrum and KS entropy. In addition, controlling chaos in physical systems has been an active area where Lyapunov-exponents can be applied to confirm the existence of controlled orbits on attractors [9]. Therefore the Lyapunov exponent is the most useful dynamical diagnosis for studying chaos and turbulence in plasmas. However, it is difficult to get a reliable Lyapunov-exponent spectrum from noisy experimental data. The identification of a quasiperiodic attractor by a Lyapunov-exponent spectrum especially becomes more difficult because of noise.

Recently a Lyapunov-exponent spectrum has been estimated in some experimental studies of plasma chaos [3,10,11]. The reliability of estimating Lyapunov exponents depends on the practical algorithm. In this paper, we would like to present a practical algorithm to estimate the Lyapunov exponents from time series signals. This algorithm is based on the works of Eckmann et al. [12] and Sano and Sawada [13] with some modification of technical details. This algorithm has been verified by several known model systems with much attention to the effect of noise on calculated Lyapunov exponents. A p-average method and a local filter technique are suggested to suppress the noise. By using this algorithm, we have distinguished quasiperiodic attractors from chaotic and periodic attractors in both computer and laboratory experiments, and confirmed a quasiperiodic transition to chaos observed in an undriven plasma [3].

II. BASIC ALGORITHM OF LYAPUNOV EXPONENT

The calculation of a Lyapunov-exponent spectrum is relatively easy for known model systems since the algorithm based on a theorem demonstrated by Oseledec [14] was proposed by Benetinn et al. [15]. However, it is difficult to calculate it from time series of experimental signals, especially from low precise and noisy data. Wright [16] and Wolf et al. [17] proposed different methods to calculate one or two positive exponents from experimental data. Eckmann et al. [12] and Sano and Sawada [13] developed similar procedures to compute the whole Lyapunov-exponent spectrum (including positive, zero, and negative exponents). Recently, several authors [18,19] have introduced further improvements of the algorithm of Eckmann et al. However, all of these algorithms require data of high precision and absence of noise. Zeng, Eykholt, and Pielke [20] have recently proposed an approach for estimating the Lyapunov exponents from rel-

atively short time series of low precision. But the error bars of zero exponents for noisy signal are not small enough to diagnose quasiperiodic attractors and strange nonchaotic attractors or otherwise clearly. Motivated by all of the works mentioned above, we present a practical algorithm to extract the Lyapunov exponents from real experimental data with noise. The basic steps of our algorithm are as follows.

(1) *Reconstruct a finite-dimensional phase space from time series.* Choose an appropriate embedding dimension d_E and a delay time τ to reconstruct a d_E-dimensional phase space by the time delay method [21] from time series $x_i = x(i\Delta t)$ ($i = 1, 2, \ldots, N$). The multivariate vectors in d_E-dimension space,

$$\mathbf{x}_i = (x_i, x_{i+m}, \ldots, x_{i+(d_E-1)m}) \, ,$$

are used to trace out the orbit of the system, where $i = 1, 2, \ldots, N - d_E + 1$, $\tau = m\Delta t$, Δt is the sampling time interval, and N is the total number of data points.

(2) *Recover the tangent maps by the least squares fitting method.* A ball of radius r is selected at each central point $\mathbf{x}_i$. Tracking the whole attractor, we search for the points $\mathbf{x}_{S_i(j)}$ ($j = 1, \ldots, p$) which are located within this ball, and call them neighbors of the points $\mathbf{x}_i$ (p is the number of neighbors). When $\mathbf{x}_i$ evolves into $\mathbf{x}_{i+n}$, the neighbors evolve into $\mathbf{x}_{S_i(j)+n}$ (in this paper, a special case $n = m$ is set). Considering the maps (yet unknown) $\mathbf{x}_{i+n} = \mathbf{F}(\mathbf{x}_i)$, we expand $\mathbf{F}$ in a Taylor series about $\mathbf{x}_i$,

$$\begin{aligned}
\mathbf{y}_{S_i(j)+n} &= \mathbf{x}_{S_i(j)+n} - \mathbf{x}_{i+n} \\
&= \mathbf{F}(\mathbf{x}_{S_i(j)}) - \mathbf{F}(\mathbf{x}_i) \\
&= \mathbf{DF}_i \cdot \mathbf{y}_{S_i(j)} + \frac{1}{2!}\mathbf{DF}_i^{(2)} : (\mathbf{y}_{S_i(j)}\mathbf{y}_{S_i(j)}) + \cdots
\end{aligned}$$

where $\mathbf{DF}_i^{(2)}$ are third rank tensors.

When the radius r is relatively small, the local linear tangent maps can be used [19]. That means

$$\mathbf{y}_{S_i(j)+n} \approx \mathbf{DF}_i \cdot \mathbf{y}_{S_i(j)} \, .$$

The $\mathbf{DF}_i$ can be regarded as the local Jacobian of $\mathbf{x}_i$. The elements of the Jacobian are determined using the least-squares error method [13].

(3) *Calculate Lyapunov exponents from the Jacobian.* By **QR** decomposition [12], the Jacobians $\mathbf{DF}_i$ are transformed to $\mathbf{Q}_i$ and $\mathbf{R}_i$ ($\mathbf{Q}_0 = \mathbf{I}$, $\mathbf{DF}_i \cdot \mathbf{Q}_{i-1} = \mathbf{Q}_i \cdot \mathbf{R}_i$), where $\mathbf{Q}_i$ are orthodox matrices and $\mathbf{R}_i$ are upper triangle matrices. Then the Lyapunov exponents λ_i are given by

$$\lambda_i = \frac{1}{M\tau} \sum_{j=1}^{M} \ln(\mathbf{R}_j)_{ii}, \quad i = 1, \ldots, d_E$$

where $M \leq (N - d_E m + 1)/m$ is the available number of the Jacobian.

III. IMPLEMENTAL DETAILS AND RESULTS OF NUMERICAL EXPERIMENTS

The basic procedure of our method for estimating Lyapunov exponents is given in the preceding section, and it

basically is similar to that of Refs. [12,13,20]. However, the precision of Lyapunov exponents depends on practical algorithms and their implemental details. Moreover, it is also known that many factors, such as noise, can hinder the successful application of the exponent extraction algorithms. In this section, we address several issues related to the accurate extraction of Lyapunov exponents from time series of low precision.

A. The best embedding dimension d_E and time delay τ

To implement this algorithm successfully, several reconstruction parameters (e.g., the best embedding dimension d_E, time delay τ) should be chosen cautiously. The embedding dimension d cannot be too large because it can lead to spurious exponents. It also enhances the problem of contamination by round-off or instrumental error since the "noise" will populate and dominate the additional $d - d_E$ dimensions of the embedding space where no dynamics operate. On the other hand, when attractor reconstruction is performed in an embedding space whose dimension is too small, a "catastrophe" that interleaves distinct parts of the attractor is likely to result. Therefore it is important to select the embedding dimension as low as possible, subject to the condition that trajectories will not intersect each other on the attractor. The well known criterion of Mañé and Takens, $d_E \geq 2d_A + 1$, is only a sufficient condition for the reconstruction of a d_A-dimensional attractor via Takens's theorem. The usual method to choose the best embedding dimension is to compute some invariants on the attractor. For example, we can determine d_E by noting when the calculated value of the correlation dimension starts saturating with increase of the embedding dimension used for computation. However, the problem with this method is that it is certainly subjective and it takes more data and more computation time to calculate d_E than to estimate the Lyapunov exponents [22]. Here we apply the "false nearest neighbors" algorithm suggested by Kennel *et al.* [23] to select the d_E directly. The basic idea is that in the passage from dimension d to dimension $d + 1$, one can differentiate between points on the orbit $\mathbf{x}_i$ that are "true" neighbors and those that are "false" neighbors which appear to be neighbors because embedding space is too small ($d < d_E$). A natural criterion for identifying false nearest neighbors is that the increase in Euclidean distance between the point $\mathbf{x}_i$ and the rth nearest neighbor $\mathbf{x}_i^r$ is large when going from dimension d to $d + 1$. We state this criterion by declaring as a false neighbor for which

$$\left[\frac{R_{d+1}^2(i, r) - R_d^2(i, r)}{R_d^2(i, r)/d} \right]^{1/2} > R_{tol}$$

where $R_d^2(i, r) = \sum_{j=0}^{d-1}[x_{i+jm} - x_{i+jm}^r]^2$ is the square of the distance between $\mathbf{x}_i$ and $\mathbf{x}_i^r$ and R_{tol} is some threshold. In our numerical investigation below, the threshold is taken to be $R_{tol} \geq 30$ and only the nearest neighbors ($r = 1$) are considered, as Kennel *et al.* proposed. We

examine every point on the orbit to count how many of the nearest neighbors are false and record the results of computations as the proportion of all points on the orbit which have a false nearest neighbor. When the percentage of the false nearest neighbors first drops to zero, the attractors are unfolded properly in a d-dimension phase space. Thus this dimension d is chosen as the best embedding dimension d_E. It should be noticed that the method is not only quite different from the nearest neighbor (NN) approach [23] but also the criterion given above is a little different from that proposed by Kennel *et al.* In fact, the criterion of Kennel *et al.* fails to determine a proper embedding dimension for white noise (a high-dimensional signal) due to the dependence of their criterion on the dimension d, and it needs a second criterion system with the limited size of the data set. On the contrary, the criterion we use is independent of the dimension d and the point which does not have a "neighbor" [that is, $R_d(i,1)/d > 0.1L$, where L is the horizontal extent of the attractor] is not taken into account. So the modified criterion can be used to determine the best embedding dimension for both low- and high-dimensional chaos, with little trouble and quite efficiently. For a time series from the Lorenz equation with additional noise, the proportion of false nearest neighbors (FNNP) is plotted against the embedding dimension as shown in Fig. 1. For a low-dimension experimental chaotic attractor as reported before [3], the result in Fig. 2 shows that the best embedding dimension d_E is 4, which has a qualitative agreement with the estimation from the saturation dimension method. For a hyperchaotic attractor with two positive Lyapunov exponents, the best embedding dimension d_E could be estimated to be 5 or 6. Clearly the saturation dimension method is invalid, as for the hy-
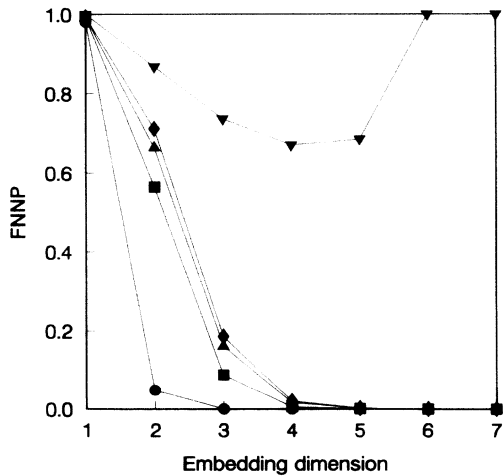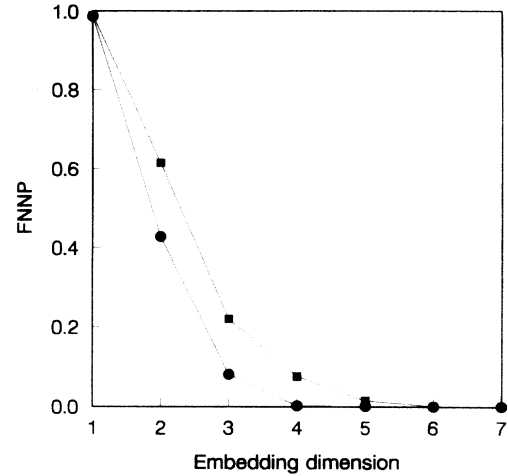

FIG. 2. The estimations of the best embedding of time series from experimental signal using the "false nearest neighbors" method. R_{tol} is the same as in Fig. 1. The filled circles show the result for a low-dimension chaotic attractor. The filled squares show the result for a hyperchaotic attractor with two positive Lyapunov exponents.

perchaotic attractor. In this way less data (≤ 5000) are required for the estimation of the embedding dimension of the low-dimension attractor. This method is very useful for the estimation of the Lyapunov exponent when one hopes to extract the exponent spectrum from the short time series quickly.

The delay time τ can, in principle, be chosen almost arbitrarily in the limit of an infinite amount of noise-free data. However, in the more likely event of a limited amount of noisy data, the choice of τ is of considerable importance in trying to reconstruct the attractor because the quality of the analysis depends on the value chosen for τ. Three methods, i.e., the space-filling method, autocorrelation function method, and average mutual information method, have been suggested for obtaining τ. However, since it is still a matter of trial and error to determine the best τ [5], in this paper τ is taken to be the lag time at which the autocorrelation function of the time series first falls to e^{-1}.

B. Radius r and neighbor number p

In the approach of estimating exponents, the choice of the radius r is a compromise between two conflicting requirements: take r sufficiently small so that the effect of nonlinearity can be neglected, but take r sufficiently large so that the ball around $\mathbf{x}_i$ contains enough neighbors for unambiguous determination of the matrix $\mathbf{DF}_i$. In our algorithm we take $r=(0.05$–$0.10)L$, where L is the horizontal extent of the attractor. When the number of one point's neighbors is too small we drop it and count for the next point, but we have found that is seldom necessary.

Next we discuss the selection of the number of neigh-

FIG. 1. The estimation of the best embedding dimension of time series using the "false nearest neighbors" method. The time series is generated from the Lorenz model with additional white noise. The noise standard deviations are 0, 10%, 30%, and 100% for filled circles, filled squares, filled triangles, and filled rhombs. The filled upper triangles present results of pure white noise. The R_{tol} used in this method is chosen as 35. "FNNP" represents the false nearest neighbor proportion.

bors p around the fiducial point $\mathbf{x}_i$. Since there are d_E unknown independent elements of the matrix $\mathbf{DF}_i$, we need at least $d_E + 1$ neighbors for the least-squares fit. Moreover, to obtain good statistics it is, of course, desirable to have a large number of neighbors. However, for a large number of p, large data sets and more computation time are required. Therefore in practice p is always given to be appropriately larger than d_E to make a compromise among limitations due to statistics and limitations due to data sets and time consumption in computation. Eckmann et $al.$ have taken $p \geq \min(d_E + 4, 2d_E)$ as a criterion for choosing the number of neighbors, and in the algorithm of Zeng et $al.$ p is given to be 10 for embedding dimension $d_E \leq 5$. As for the behavior of the first exponent with increasing p in our numerical experiments which is shown in Fig. 3(a), in our algorithm, we have selected p as follows. We first choose $p_{\min} = 2\min(d_E + 4, 2d_E)$ and count the number of neighbors of $\mathbf{x}_i$ corresponding to increasing values of $p \geq p_{\min}$. If the number of neighbors around the point $\mathbf{x}_i$ is less than the preselected value p, we drop this point $\mathbf{x}_i$ and proceed to the next point $\mathbf{x}_{i+n}$. When the proportion of dropped points is larger than a threshold, for example, 2% of the total number of points which have been used, we stop increasing p and take this value of p as $p_{\max}$. Then Lyapunov exponents calculated for different values between $p_{\min}$ and $p_{\max}$ are averaged. Using the p-average method, we also study the first Lyapunov exponent of the Lorenz system as the function of the precision of data, with a range from 6 bits to 16 bits. As shown in Fig. 3(b), when the precision of data is only 6 bits, the relative errors is 3%. By increasing the precision, the relative error is quite small, for 8 bits only 1–2%. This implies that our algorithm is not so sensitive to the precision of data on the estimation of Lyapunov exponents. In the next section it is shown that by this p-average method, the influence of noise can be suppressed significantly.

C. Effect of noise on the estimation of exponents

Furthermore, the noise will take an important role in the estimation of the Lyapunov exponent. When Gaussian noise is added into the Lorenz time series, the first Lyapunov exponent is almost proportional to noise deviation (shown in Fig. 4). Before use of the p-average method, the first Lyapunov exponent is quite different from the accepted one, even the noise deviation $\Delta_n \leq 5\%$ (shown as filled triangles). Using the p-average method, the relative error between the computed first Lyapunov exponent and the accepted one has been reduced significantly for $\Delta_n \leq 5\%$ (shown as filled circles). However, the problem still remains open for $\Delta_n > 5\%$ even though a shell [12,20] is selected to minimize the noise in our algorithm. In most of our experiments, $\Delta_n < 5\%$ [3], the Lyapunov exponents can be estimated relatively accurately by the p-average method. It is worth investigating how to extract the Lyapunov exponent from time series with $\Delta_n > 5\%$. In performing the calculation of the Lyapunov exponent a small ball radius is required for fitting the local Jacobian matrix, however, when $|\mathbf{x}_{S_i(j)+n} - \mathbf{x}_{i+n}|$ is so small that the noise effect becomes the greatest one to result in the unreliable Lyapunov exponent. Therefore the time series signal $x(i\Delta t)$ has to be filtered before the reconstruction of a finite-dimension phase space. Here a local filter method is suggested to suppress the noise in the time series signal. The conceptually simple, local filter method [24] with the help of interpolations is as follows. Let $f_j(t)$ be a cubic spine through every Jth point $x[(j + iJ)\Delta t], i = 0, 1, \ldots$ starting from the jth one. The smoothed time series is obtained by the average of these

FIG. 4. The first Lyapunov exponent of the Lorenz system as the function of the deviation of Gauss noise included in time series. The filled triangles show these results without using the p-average and local filter methods, the results using the p-average method without filter are shown as these filled circles, and the filled squares refer to those results computed by using the p-average method and prefilter performance. As $\Delta_n \leq 5\%$, p average is a quite useful method. For $\Delta_n > 5\%$, an improvement has been achieved clearly when the local filter method is used.
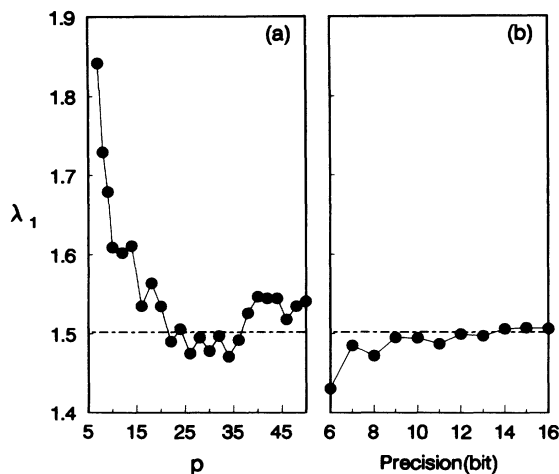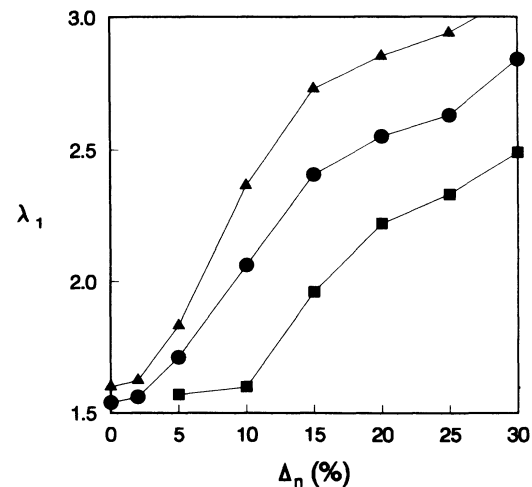

FIG. 3. The first Lyapunov exponent of the Lorenz system as (a) the function of the number of neighbors p; (b) the precision of data. The dashed lines in (a) and (b) refer to the accepted value 1.50. The parameter r is chosen as $0.05L$ for (a) and (b), and $\tau = 0.2$.

spines at the time nodes,

$$x^* = \frac{1}{J} \sum_{j=1}^{J} f_j(t) \ ,$$

where $x^* = x^*(n\Delta t)$ is a filtered time series signals. It is hoped that Lyapunov exponents of the dynamical system are less affected by the local filter method. Therefore J is selected carefully to avoid the changes of the original attractor.

First, for given Lorenz time series including Gaussian noise ($\Delta_n \sim 5 - 30\%$), after the Lorenz times series including noise are filtered, the practical algorithm mentioned above is applied to the filtered data. The results are compared with the reported Lyapunov exponent. We found that $K = 2$–10 could give satisfactory results. In Fig. 4, the filled squares represent the estimation of the first Lyapunov exponent with the local filter technique. It is clear that the filter technique has improved the estimation of Lyapunov exponents although the strong noise still makes the value of the Lyapunov exponent rather larger than the reported one. The detailed discussion on noise reduction will be published elsewhere.

D. Numerical results on known models

Using the practical algorithm discussed above, we calculated the Lyapunov-exponent spectra from the time series of some known systems such as Lorenz, Rössler, and Mackey-Glass. Lorenz data were generated from the Lorenz system of equations:

$$\dot{x} = \sigma(y - x) \ ,$$
$$\dot{y} = cx - y - xz \ ,$$
$$\dot{z} = -bz + xy \ ,$$

where $\sigma = 16$, $b = 4.0$, $R = 45.92$. In generating the Lorenz data we used a Runge-Kutta integration step size 0.005 and a sampling interval $\Delta t = 0.02$. Rössler data were generated from the Rössler equations:

$$\dot{x} = -z - y \ ,$$
$$\dot{y} = x + ay \ ,$$
$$\dot{z} = b + z(x - c) \ ,$$

where $a = b = 0.2$, $c = 10.0$. The integration step size is 0.05 and the sampling interval $\Delta t = 0.2$. The Mackey-Glass data were generated from the Mackey-Glass delay-differential equation:

$$\dot{x}(t) = \frac{ax(t - T)}{1 + x(t - T)^c} - bx(t) \ ,$$

where $a = 0.2$, $b = 0.1$, $c = 10$, $T = 30$. The integrating step is $0.005T$ and the sampling interval $\Delta t = 0.03T$ ($T = 30$). In order to apply our algorithm to experimental signals, the elements of time series x_i are transferred to integers ranging from 0 to 255. The error bars, shown in Table I, are computed from a few runs with changes of r (radius) and τ. All the error bars are relatively small. For the Lorenz system, difference between the computed largest exponent λ_1 and the accepted value is less than 3%. Since the λ_2 is only 2% of λ_1 and at least one exponent must be zero, we can regard λ_2 as zero in spite of its error bar. For the Rössler system, λ_1 is obtained with a relative error less than 3%, and λ_2 is less than 3% of λ_1. For the Mackey-Glass equation, relative errors of λ_1, λ_2 are about 4% and 25%, and the computed D_{KY} is 3.53, which is similar to the accepted 3.59. The possibility of measuring negative exponents depends on their magnitudes and the signal-to-noise ratio of the data [13]. Because the precision of 8 bits is prescribed, as shown

TABLE I. Lyapunov-exponent spectra for several known systems. The entropy K_2 and D_{KY} estimated from the Lyapunov-exponent spectrum are also given in the table.

Model	Accepted λ_i	Computed λ_i
Lorenz	1.50 [17]	1.54±0.08
(σ=16,b=4.0,R=45.92)	0.00	0.03±0.21
(τ=0.2,N=8000)	−22.46	−3.70±0.42
	K_2=1.50	K_2=1.54
	D_{KY}=2.06	D_{KY}=2.42
Rössler	0.069±0.003 [13]	0.069±0.002
($a = b = 0.2, c = 10$)	−0.0002±0.0003	−0.002±0.004
($\tau = 1.2, N = 8000$)	−4.978±0.02	−0.88±0.05
	$K_2 = 0.069$	$K_2 = 0.069$
	D_{KY}=2.01	D_{KY}=2.08
Mackey-Glass	0.0071 [13]	0.0068±0.0002
($a = 0.2, b = 0.1, c = 10, T = 30$)	0.0027	0.0020±0.0003
(τ=13.5,N=16000)	0.000	−0.0023±0.0004
	−0.0167	−0.0123±0.003
	−0.0245	−0.0304± 0.0009
	K_2=0.0098	K_2=0.0088
	D_{KY}=3.59	D_{KY}=3.53

in Table I, $|\lambda_3| \geq 100|\lambda_1|$ for the Rössler system and $|\lambda_3| \geq 15|\lambda_1|$ for the Lorenz system, the computed exponent $|\lambda_3|$ is very small compared with the reported one. However, when the absolute values of the negative exponents are comparable with the largest positive exponent, as for the Mackey-Glass system, computed negative exponents are comparable to the accepted ones.

In addition, we have also calculated the Lyapunov-exponent spectra of the two- and three-frequency quasiperiodic and strange nonchaotic time series including white noise (standard deviation 10%) that are generated from quasiperiodic driven damped pendulum [4].

$$\frac{1}{p}\frac{d^2\phi}{dt^2} + \frac{d\phi}{dt} - \cos\phi = K + V(\cos\omega_1 t + \cos\omega_2 t) ,$$

where $\omega_1 = 1$, $\omega_2 = (\sqrt{5} - 1)/2$, $p = 3.0$, and $V = 0.55$. All the calculated results are included in Table II. For a two-frequency quasiperiodic attractor (K=1.34), the calculated Lyapunov exponent spectrum, $|\lambda_1| \sim |\lambda_2| < 0.16|\lambda_3|$, can be regarded as $(0, 0, -)$. For a given three-frequency quasiperiodic attractor $(K=1.77)$, the calculated Lyapunov-exponent spectrum, $\max(|\lambda_1|, |\lambda_2|, |\lambda_3|) < 0.18|\lambda_4|$, is regarded as $(0, 0, 0, -)$. For a strange nonchaotic attractor $(K = 1.33)$, the calculated Lyapunov-exponent spectrum, $|\lambda_1| \sim |\lambda_2| < 0.2|\lambda_3|$, can be regarded as $(0, 0, -)$. It is worth mentioning that noise included in quasiperiodic attractors could be removed by the local filter method, and a quasiperiodic attractor almost is kept unchanged after the filter. Therefore a quasiperiodic attractor can indeed be confirmed in the experiments by the Lyapunov-exponent spectrum. However, the filter technique has to be carefully used for the chaotic attractor, because the filter might change the chaotic attractor a little.

After the verification mentioned above, it is confirmed that our algorithm can not only estimate the Lyapunov exponents of chaotic time series but also distinguish the quasiperiodic experimental signals from the chaotic and the periodic experimental signals.

TABLE II. Lyapunov-exponent spectra for two-frequency quasiperiodic, three-frequency quasiperiodic and strange nonchaotic attractors with white noise (standard deviation 10%). The attractors are generated from a quasiperiodic driven damped pendulum with different values of K [4]. (The sampling time interval $\Delta t = \pi/25$, $\tau = 10$–$20\Delta t$.)

Type of attractor	λ_i from equation	λ_i from time series
two-frequency	0.000	0.034 ± 0.02
quasiperiodic	0.000	-0.039 ± 0.02
$(K = 1.34, N = 8000)$	-0.239	-0.210 ± 0.03
three-frequency	0.000	0.047 ± 0.03
quasiperiodic	0.000	-0.001 ± 0.02
$(K = 1.77, N = 16000)$	0.000	-0.055 ± 0.03
	-3.000	-0.30 ± 0.10
strange nonchaotic	0.000	0.034 ± 0.02
$(K = 1.33, N = 8000)$	0.000	-0.037 ± 0.02
	-0.158	-0.180 ± 0.03

IV. LYAPUNOV-EXPONENT SPECTRUM OF EXPERIMENTAL PLASMA CHAOS

We have applied the algorithm to experimental data of the undriven chaotic plasma system. A quasiperiodic transition to chaos in undriven plasma has been investigated experimentally (Ding et al. [3]). Plasma is produced by argon gas direct current discharged between the anode and the hot cathode. Typical plasma electron density $n_e = 10^8$–10^9 cm^{-3}, electron temperature $T_e = 1$–3 eV, $T_i \ll T_e$. The signals of discharge current $I_D(t)$ are recorded by digitizers (data precision 8 bits, data size $N=8192$). The quasiperiodic transition to chaos can be found by varying the gas pressure P_a when a periodic oscillation is initiated by varying the discharge voltage V_D. The computation of Lyapunov exponents for experimental data has been summarized in Table III for different controlling parameters P_a. At $P_a = 7.9 \times 10^{-4}$ torr, since at least one of the exponents must be zero, we can recognize λ_1 as zero (well within the error bars). So the case is easily identified as $(0, -, -)$ which indicates that the plasma is in the periodic state. Similarly, the exponents for $P_a = 8.0 \times 10^{-4}$ torr are identified as $(0, 0, -, -)$ (since $|\lambda_1| \approx |\lambda_2| \ll |\lambda_3|, |\lambda_4|$) which indicates the appearance of the quasiperiodic state. One for $P_a = 8.1 \times 10^{-4}$ torr as $(+, 0, -, -)$ indicates the chaotic state (the detailed experimental results can be seen in Ref. [3]). Finally, we show in Table III the estimations of Kolmogorov entropy K_2 and dimension $D_{KY} = 2.86$ which can be compared to the correlation dimension $D_2 = 2.90 \pm 0.02$ by using the Grassberger-Procaccia algorithm [25]. In our experiments usually the noise level is less than 5%. When the modified algorithm (p average) is applied to experimental data the leading Lyapunov exponent can be improved 10% without the local filter method. Furthermore, in order to distinguish the quasiperiodic attractor we use the local filter method for the experimental data related to the quasiperiodic attractor. In this situation we hope to get two comparable zero Lyapunov exponents which indicate a quasiperiodic attractor. Without the local filter method it is difficult to confirm an experimental quasiperiodic attractor. It should be noticed that the local filter method might change the original chaotic attractor a little and almost does not change the quasiperiodic attractor.

V. DISCUSSIONS AND CONCLUSIONS

A full Lyapunov-exponent spectrum in nonlinear dynamical experiments is important to distinguish different attractors. The practical algorithm presented has been tested on several known models (e.g., Lorenz, Rösseler) and has been found efficiently and reliably. In order to avoid spurious exponents the false nearest neighbors method is used to select the best embedding dimension d_E directly. Compared with the calculations of correlation dimension, the false nearest neighbors method is performed with relatively little data and less computing time is consumed. The estimation of the best embedding

TABLE III. Lyapunov-exponent spectra for different plasma states at $P_a = 7.9, 8.0, 8.1 \times 10^{-4}$ torr, respectively. These results clearly indicate a quasiperiodic transition to chaos in a plasma.

$P_{Ar}(10^{-4}$ torr)	λ_1	λ_2	λ_3	λ_4	K_2 entropy	D_{KY}
7.9	−0.022	−1.503	−3.467			
8.0	0.069	−0.054	−1.322	−2.434		
8.1	1.069	−0.080	−1.148	−3.363	1.069	2.86

dimension can be accepted for the data masked by up to 30% noise. The influence of noise on the best embedding dimension is much less than on the Lyapunov exponents. Although the determination of time delay τ remains controversial, the method of autocorrelation function could be applied for our practical uses. Our algorithm is mainly influenced by the appearance of the noise. For noise less than 5%, a p-average method which we suggest in this paper can be used to obtain relatively accurate results. For larger noise, a local filter technique has to be applied to time series before the reconstruction of phase space. Although removing noise from chaotic signals is a challenging problem which has not been solved completely, anyway, an improvement of the estimation of the Lyapunov-exponent spectrum has been achieved in our performance with the help of a local filter. In order to apply our algorithm to verify quasiperiodic and strange nonchaotic attractors, we have also computed the Lyapunov-exponent spectra from the time series of two-frequency and three-frequency quasiperiodic and strange nonchaotic attractors. Fortunately, Lyapunov exponents found by means of the phase space reconstruction technique are in agreement with those found by solving the equation directly. Furthermore, the algorithm has been applied to real experimental data in the chaotic system of undriven plasma [3], and the computed results correspondent to that of power spectrum analysis and phase space portrait very well. The calculation of Lyapunov exponents quantitatively characterizes an experimental quasiperiodic transition to chaos in an undriven plasma. It is hoped that the practical algorithm presented here has wide applicability to research on plasma chaos, turbulence, and transport properties where the dynamics equations might not be available.

ACKNOWLEDGMENTS

[1] P.Y. Cheung and A.Y. Wong, Phys. Rev. Lett. **59**, 551 (1987); see also P.Y. Cheung, S. Donovan, and A.Y. Wong, ibid. **61**, 1360 (1988).

[2] Jiang Yong, Wang Haida, and C.X.Yu, Chin. Phys. Lett. **5**, 489 (1988); J. Qin, L. Wang, D.P. Yuan, P. Gao, and B.Z. Zhang, Phys. Rev. Lett. **63**, 163 (1989).

[3] Ding Weixing, Huang Wei, Wang Xiaodong, and C.X. Yu, Phys. Rev. Lett. **70**, 170 (1993).

[4] The strange nonchaotic attractor found by Grebogi et al. offers some very interesting dynamical properties. Consequently, a strange nonchaotic attractor is an attractor that is geometrically strange, but for which nearby trajectories do not diverge exponentially. Its Lyapunov-exponent spectrum is the same as that of quasiperiodicity. There are several characterizations of it in numerical experiments such as surface section, spectrum distribution function, fractal dimension, and Lyapunov-exponent spectrum. However, in most experimental circumstances, the most useful characterization is the Lyapunov-exponent spectrum together with correlation dimension. For a detailed discussion of the strange nonchaotic attractor see C. Grebogi, E. Ott, S. Pelikan, and J.A. Yorke, Physica D **13**, 261 (1985); A. Bondeson, E. Ott, and T.M. Antonsen, Phys. Rev. Lett. **55**, 2103 (1985); F.J. Romeiras, A. Bondeson, E. Ott, T.M. Antonsen, and C. Grebogi, Physica D **26**, 277 (1987); F.J. Romeiras and E. Ott, Phys. Rev. A **35**, 4404 (1987); M. Ding, C. Grebogi, and E. Ott, Phys. Rev. A **39**, 2593 (1989); Phys. Lett. A **137**, 167 (1989). The experiments on the strange nonchaotic attractor are described in W.L. Ditto, M.L. Spano, H.T. Savage, S.N. Rauseo, J. Heagy, and E. Ott, Phys. Rev. Lett. **65**, 533 (1990); W. Huang, B.S. thesis, University of Science and Technology of China, 1993.

[5] Hao Bai-lin, Elementary Symbolic Dynamics (World Scientific, Singapore, 1989).

[6] A.N. Kolmogorov, Dokl. Akad. Nauk. SSSR **119**, 861 (1958) [Sov. Phys. Dokl. **112**, 426 (1958)].

[7] P. Fredrickson, J.L. Kaplan, E.D. Yorke, and J.A. Yorke, J. Differ. Eq. **49**, 185 (1983).

[8] P. Gaspard and G. Nicolis, Phys. Rev. Lett. **65**, 1693 (1990).

[9] W.X. Ding, H.Q. She, W. Huang, and C.X. Yu, Phys. Rev. Lett. **72**, 96 (1994).

[10] N. Ohno, A. Komori, M. Kono, and Y. Kawai, Phys. Fluids B **5**, 796 (1993).

[11] T. Klinger and A. Piel, Phys. Fluids B **4**, 3900 (1992).

[12] J.-P. Eckmann, S. Oliffsion Kamphorst, D. Ruelle, and S. Ciliberto, Phys. Rev. A **34**, 4971 (1986); also see J.-P. Eckmann and D Ruelle, Rev. Mod. Phys. **57**, 617 (1985).

[13] M. Sano and Y. Sawada, Phys. Rev. Lett. **55**, 1082 (1985).

[14] V.I. Oseledec, Trans. Mosc. Math. Soc. **19**, 17 (1968).

[15] G. Benetinn, L. Galani, A. Giorgilli, and J.-M. Strelcyn, Meccanica **15**, 9 (1980).

[16] J. Wright, Phys. Rev. A **29**, 2923 (1984).

[17] A. Wolf, J.B. Swift, H.L. Swinney, and J.A. Vastano, Physica D **16**, 285 (1985).

[18] K. Briggs, Phys. Lett. A **151**, 27 (1990).

[19] R. Brown, P. Bryant, and H.D.I. Abarbanel used high order maps: Phys. Rev. A **43**, 2787 (1991); Phys. Rev. Lett. **65**, 1523 (1990).

[20] X. Zeng, R. Eykholt, and R.A. Pielke, Phys. Rev. Lett. **66**, 3229 (1991); also see X. Zeng, R.A. Pielke, and R. Eykholt, Mod. Phys. Lett. B **6**, 55 (1992).

[21] N.H. Packard, J.P. Crutchfield, J.D. Farmer, and R.S. Shaw, Phys. Rev. Lett. **45**, 712 (1980); see also F. Takens, in *Dynamical Systems and Turbulence* (Springer-Verlag, New York, 1981), p. 366.

[22] D. Ruelle, Proc. R. Soc. London, Ser. A **427**, 241 (1990).

[23] M.B. Kennel, R. Brown, and H.D.I. Abarbanel, Phys. Rev. A **45**, 3403 (1992). This FNNP approach here to estimate the best embedding dimension is quite different from the NN approach to local intrinsic dimension [see it in M.E. Farrel, A. Passamante, and T. Hediger, Phys. Rev. A **41**, 6591 (1990)] at least in two aspects. The first, the FNNP approach, gives an estimation of the dimension of phase space in which the attractor is embedded, while the NN approach gives an estimation of the attractor and its result is an upper bound on the correlation dimension and a lower bound on the information dimension and Housdorff dimension. It is clear that the best embedding dimension (BED) is larger than the local intrinsic dimension (LID). The second, the FNNP method modified by us, is not as sensitive to noise [even if the signal-to-noise ratio (SNR) is down to 0 dB, the BED can be accepted; see Fig. 1], and the NN approach works only in the case of little or no additive noise (SNR $\geq$ 30 dB). In general, the FNNP approach is more practical to estimate the Lyapunov-exponent spectrum.

[24] B.R. Noack, F. Ohle, and H. Eckelmann, Physica D **56**, 389 (1992).

[25] P. Grassberger and I. Procaccia, Phys. Rev. Lett. **50**, 346 (1983).